

Enantiopure five-membered cyclicdiamine derivatives as potent and selective inhibitors of factor Xa. Improving in vitro metabolic stability via core modifications

Jennifer X. Qiao,* Tammy C. Wang, Gren Z. Wang, Daniel L. Cheney, Kan He, Alan R. Rendina, Baomin Xin, Joseph M. Luetzgen, Robert M. Knabb, Ruth R. Wexler and Patrick Y. S. Lam

Bristol-Myers Squibb Company, Research and Development, PO Box 5400, Princeton, NJ 08643-5400, USA

Received 3 June 2007; revised 4 July 2007; accepted 6 July 2007

Available online 13 July 2007

Abstract—We previously reported a series of enantiopure *cis*-(1*R*,2*S*)-cyclopentylidiamine derivatives as potent and selective inhibitors of Factor Xa (FXa). Herein, we describe our approach to improve the metabolic stability of this series via core modifications. Multiple resulting series of compounds demonstrated similarly high FXa potency and improved metabolic stability in human liver microsomes compared with the cyclopentylidiamide **1**. (3*R*,4*S*)-Pyrrolidinyldiamide **31** was the best overall compound with human FXa K_i of 0.50 nM, PT EC_{2x} of 2.1 μ M in human plasma, bioavailability of 25% and $t_{1/2}$ of 2.7 h in dogs. Further biochemical characterization of compound **31** is also presented.

© 2007 Elsevier Ltd. All rights reserved.

Factor Xa (FXa), a serine protease located at the convergent point of the intrinsic and extrinsic pathways, binds phospholipids, cofactor VIIIa, and calcium ions to form a prothrombin complex, which is responsible for catalyzing the conversion of prothrombin to thrombin. A promising strategy to develop novel anticoagulants is to inhibit thrombin formation via the inhibition of FXa.^{1–3} Several small-molecule, orally active FXa inhibitors, including pyrazole-based razaxaban⁴ and apixaban,⁵ have entered clinical development for the treatment and prevention of thrombotic diseases, and apixaban is undergoing evaluation in phase 3 studies in various indications.

In a previous communication,⁶ we disclosed a series of enantiopure (1*R*,2*S*)-cyclopentylidiamine derivatives as potent and selective FXa inhibitors structurally different from the pyrazole-based scaffolds. However, low metabolic stability in liver microsomal incubation studies was an issue common to this series of compounds. For instance, 79% of compound **1** bearing a chlorothiophene

P1 and a phenylpyridone P4 group⁷ remained after 10-min incubation in human liver microsomes (HLM), and **1** had a microsomal intrinsic clearance rate of 0.063 nmol/min/mg. Cyclopentylidiamine derivatives bearing several other P1 and P4 groups also displayed metabolic instability in HLM. Metabolic ID studies on compound **1** showed that 12% and 8% of **1** were monohydroxylated at the cyclopentyl ring and the phenylpyridone P4 moiety, respectively, after 1 h incubation in HLM in the presence of NADPH.

Several compounds in the cycloalkyldiamine series⁶ were tested stable to amide hydrolysis in dog plasma in vitro for up to 4 h, indicated by the sustained anti-FXa activity and HPLC peak area. In addition, no metabolites related to amide cleavage were observed during the metabolic stability studies of compound **1**.

The interactions of a ligand in the FXa S1 and S4 subsites are essential to the FXa binding affinity of the ligand. Previous SAR studies⁶ identified 5-chlorothiophene and 3-chloroindole as optimal P1 groups for FXa potency, and phenylpyridone group as the most potent neutral P4 group in the cyclopentylidiamine derivatives. Driven by our continuous interest in structurally diverse back-up series, we decided to further modify the

Keywords: Factor Xa inhibitors; Enantiopure cyclicdiamine derivatives; SAR; Human liver microsomal stability.

* Corresponding author. Tel.: +1 609 818 5298; fax: +1 609 818 6810; e-mail: jennifer.qiao@bms.com

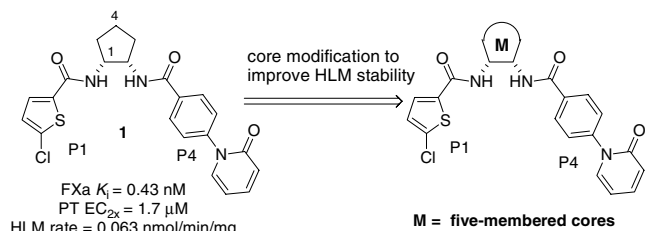


Figure 1. Overall strategy.

cyclopentyl core of the lead **1** (Fig. 1) to improve in vitro metabolic stability so as to ultimately improve the pharmacokinetic properties of this series of compounds.

Figure 2 shows an overlay of the X-ray crystal structures of compound **1**⁶ and the pyrazole-based compound **4** (apixaban)⁵ in the FXa binding site. Significant differences in binding are confined to the core region. In the **1**-FXa complex, the amide NH forms a hydrogen bond to the carbonyl oxygen of G216, whereas **4** is hydrogen bonded to G216 NH via the carbonyl oxygen of the pyrazolo pyridinone core. In the **4**-FXa complex, the C3 substituent on the pyrazole ring (CONH₂ in **4**; a variety of groups such as CF₃ are also tolerated) interacts with the S1 β pocket. The overlay shows that the 4 and the 5 positions of the cyclopentyl ring in **1** are close to the C3 substituent of **4**, suggesting that modifications on the periphery of the cyclopentyl ring in **1** could improve the properties of the molecules (e.g., to improve metabolic stability by blocking the oxidative metabolism on the cyclopentyl ring) while maintaining or improving potency. Such modifications include fusing a ring to, or adding a substituent at the 4 position of, or inserting a heteroatom at the 4 position of the cyclopentyl ring.

Indeed, fusing the cyclopentyl core with a phenyl ring led to diaminoindane analogs. Table 1 shows FXa activities of enantiopure *cis* diaminoindanes bearing either a 3-chloroindole or a 5-chlorothiophene P1 group. The two *cis* 1,2-diaminoindane enantiomers, compound **6**

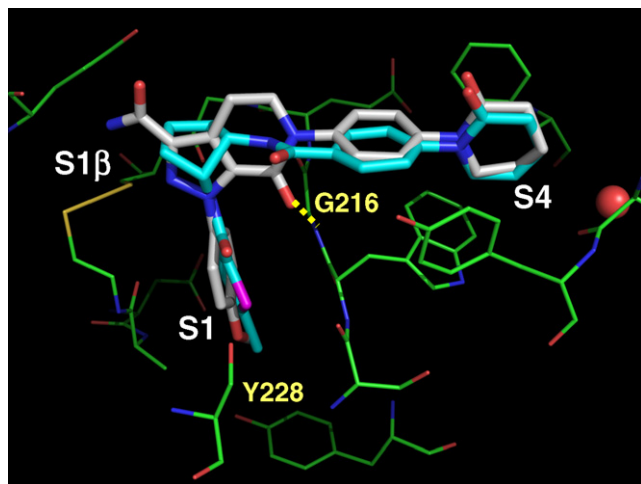


Figure 2. Overlay of X-ray structures of FXa bound *cis*-(1*R*,2*S*)-cyclopentylidiamide **1** and pyrazole bicyclic-based apixaban (**4**). Created using PyMol.⁸

Table 1. SAR of enantiopure *cis*-diaminoindane derivatives

Compound	M	P1	FXa K_i (nM)	PT EC_{2x} (μ M)
5		3-Cl-Indole-6-yl	0.70	nd
1		5-Cl-Thiophene-2-yl	0.43	1.7
6		3-Cl-Indole-6-yl	0.21	14
7		5-Cl-Thiophene-2-yl	230	nd
8		3-Cl-Indole-6-yl	0.84	5.5
9		5-Cl-Thiophene-2-yl	27	nd
10		3-Cl-Indole-6-yl	7.9	nd
11		5-Cl-Thiophene-2-yl	10870	nd
12		3-Cl-Indole-6-yl	1.0	nd
13		5-Cl-Thiophene-2-yl	0.27	3.3

Human purified enzymes were used. Values are averages from multiple determinations ($n \geq 2$). K_i values and PT EC_{2x} (the concentration of the inhibitor that doubles the prothrombin time from the control in the prothrombin time assay) values were measured as described in Ref. 9. Same for all the tables in this publication.

with a *cis*-up ((1*S*,2*R*)-2,3-dihydro-1*H*-inden-1-yl) configuration and compound **8** with a *cis*-down ((1*R*,2*S*)-2,3-dihydro-1*H*-inden-1-yl) configuration bearing a 3-chloroindole group, were potent with FXa K_i less than 1 nM. On the other hand, the corresponding two *cis* 1,2-diaminoindane enantiomers **7** and **9** bearing a 5-chlorothiophene P1 group were much less potent. Compounds **11** and **13** with a 2,1-diaminoindane core and a chlorothiophene P1 had drastically different FXa potency. Compound **11** with a *cis*-up ((1*R*,2*S*)-2,3-dihydro-1*H*-inden-2-yl) configuration was weakly active; while compound **13** with a *cis*-down configuration ((1*S*,2*R*)-2,3-dihydro-1*H*-inden-2-yl) was the most potent (FXa K_i = 0.27 nM) in the diaminoindane series, having potency similar to the parent cyclopentyl analog **1**. Compound **13**, however, was extensively metabolized in HLM (32% remaining after 10-min incubation) presumably because of the oxidation of the phenyl ring of the indane core.

Docking studies¹⁰ of the 1,2-diaminoindane (compounds **6** and **8**) and the 2,1-diaminoindane (compounds **11** and **13**) analogs were conducted to gain structural insights into the observed SAR. Figure 3 shows the overlay of the top-scoring binding models of compounds **6**

and **8**, and the X-ray structure of **1** in the active site of FXa. The corresponding P1 and P4 regions of **6** and **8** overlap very well. However, the two indane cores occupy different subsites of the FXa enzyme: the indane ring in **6** with a *cis*-up configuration sits above the 42–58 disulfide bridge, near the S1' pocket; while the indane ring in **8** with a *cis*-down configuration locates in the vicinity of the 191–220 disulfide in the S1 β region. Compared with compound **1**, the sterically demanding 1,2-diaminoindane cores of **6** and **8** tend to pull the molecules out farther away from the active site. Thus, larger P1 groups, 3-chloroindole in the case of **6** and **8**, are needed to form necessary interactions with the S1 pocket to maintain FXa potency. This also explains the decreased FXa potency observed in **7** and **9** bearing a smaller 5-chlorothiophene P1 group. Interactions in the FXa S1 β and the entrance of the S1' region may also affect FXa potency of diaminoindane compounds, as suggested by the potency difference between **7** and **9**. Figure 4 shows the proposed binding model of the 2,1-diaminoindane **13**, wherein the inversion of the cyclopentyl ring results in a reversal of the axial/equatorial orientations of the P1 and P4 groups with respect to that observed in the crystal structure of **1**-FXa. This model suggests that the core phenyl is projected into solvent well away from the protein surface, allowing the 5-chlorothiophene to bind deeply in the S1 pocket. Not surprisingly, a compelling binding model in FXa of the weakly active 2,1-diaminoindane **11** with optimal interactions could not be generated.¹¹

Adding a COOMe group on the 4 position of the cyclopentyl core in **1** generated compound **14** with maintained FXa potency and anticoagulant activity (Table 2). Reduction of the methyl ester **14** to methyl alcohol **15** led to the same affinity as the unsubstituted cyclopentane **1**. The acid **16** and the amides **17–20** had similar FXa potency and were about three to four times less potent than the methyl ester **14**. They were also less potent in anticoagulant activity. Compound **15**, the most po-

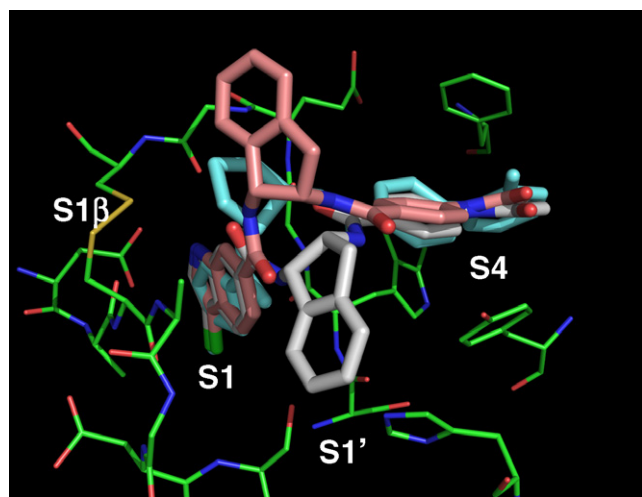


Figure 3. Overlay of binding models of two 1,2-diaminoindane enantiomers **6** (white) and **8** (pink) with the X-ray structure of cyclopentylidiamide **1** (blue) in the active site of FXa. Created using PyMol.⁸

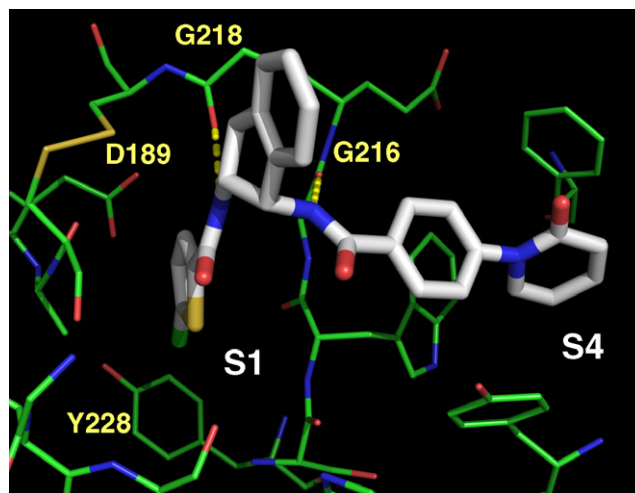


Figure 4. Binding model of the 2,1-diaminoindane **13** in the active site of FXa. Flipping of the cyclopentyl ring results in the reversal of the axial/equatorial orientations of the P1 and P4 groups with respect to that observed in the crystal structure of **1** in FXa. Created using PyMol.⁸

tent analog in the 4-substituted cyclopentyl series studied, had an improved metabolic stability (100% remaining after 10 min) compared with **1** (79% remaining).

Using the 3-chloroindole and the 5-chlorothiophene P1 groups, we investigated the FXa inhibitory activities of five-membered ring analogs (Table 3). The tetrahydrofuranyldiamine derivative **23** and the substituted pyrrolidinyldiamine derivatives **29** and **31** showed good FXa potency and anticoagulant activity. Compounds with a 5-chlorothiophene P1 group were consistently more potent than those with a 3-chloroindole group across the five-membered cores studied (4-substituted cyclopentyl, tetrahydrofuranyl, pyrrolidinyl core series). This P1 preference was also observed previously between the cyclopentylidiamine and cyclohexylidiamine

Table 2. SAR of 4-substituted cyclopentylidiamine derivatives

Compound	R	FXa	
		K_i (nM)	PT EC _{2x} (μM)
1	H	0.43	1.7
14	COOMe	0.53	1.8
15	CH ₂ OH	0.56	1.5
16	COOH	1.9	4.7
17	CONMe ₂	2.1	6.5
18	CONH-Cyclopropyl	1.6	7.1
19	CO- <i>N</i> -Morpholinyl	1.6	4.9
20	CONHCH ₂ CH ₂ OMe	2.9	4.7

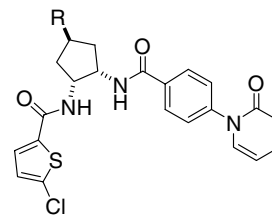
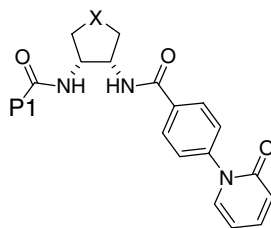


Table 3. SAR of enantiopure 4-substituted five-membered cyclicdiamine derivatives

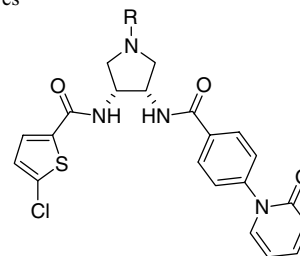
Compound	X	P1	FXa K_i (nM)	PT EC _{2x} (μM)
1	CH ₂	5-Cl-Thiophene-2-yl	0.43	1.7
5	CH ₂	3-Cl-Indole-6-yl	1.0	5.5
21	CH-COOMe	5-Cl-Thiophene	0.39	1.8
22	CH-COOMe	3-Cl-Indole-6-yl	3.0	nd
23	O	5-Cl-Thiophene-2-yl	2.6	3.2
24	O	3-Cl-Indole-6-yl	2.6	7.1
25	NH	5-Cl-Thiophene-2-yl	9.5	nd
26	NH	3-Cl-Indole-6-yl	18	nd
27	N-Fmoc	5-Cl-Thiophene-2-yl	4.5	nd
28	N-Fmoc	3-Cl-Indole-6-yl	163	nd
29	N-COMe	5-Cl-Thiophene-2-yl	0.58	0.90
30	N-COMe	3-Cl-Indole-6-yl	3.9	nd
31	N-COOEt	5-Cl-Thiophene-2-yl	0.50	2.1
32	N-COOEt	3-Cl-Indole-6-yl	2.8	nd

Comparison of two P1 groups: 5-chlorothiophene and 3-chloroindole.

derivatives.⁶ Furthermore, the more sterically demanding the X substituent, the larger the potency difference is, for example, **25** versus **26** (X = NH), twofold; while **27** versus **28** (X = N-Fmoc), 36-fold.

Using the preferred 5-chlorothiophene P1 group, R substituents on the nitrogen atom of the pyrrolidinyldiamide core were further investigated. **Table 4** demonstrates that a variety of substituents were tolerated. Neutralization of the pyrrolidine ring in **25** to form amides, carbamates, sulfonamides, and ureas resulted in improved FXa inhibitory activity (**29**, **31**, and **33–46**). Among the compounds with amide substituents, the methyl amide analog **29** (FXa K_i = 0.58 nM, PT EC_{2x} = 0.98 μM) was three to four times more potent than those with larger hydrophobic groups such as COCH₂Me, COCHMe₂, CO-*t*-Bu, CO-cyclopropyl, CO-phenyl. Polar substitution in the amide, such as CO-CH₂OMe, was tolerated, and compound **38** was equipotent to the methyl amide **29** in FXa inhibitory activity, but slightly less active in the anticoagulant activity. The methyl and ethyl carbamates **39** and **31** as well as the methyl and ethyl sulfonamides **41** and **42** were also potent FXa inhibitors (FXa K_i < 1 nM, PT EC_{2x} < 3 μM). The dimethyl urea **46** was the most potent urea analog, having a FXa K_i of 0.56 nM and a PT EC_{2x} of 1.8 μM. Similar to the amides, sulfonamides and ureas with larger alkyl groups, such as **43** bearing an isopropylsulfonamide and **44** with a pyrrolidinyl urea, were less potent than those with a smaller alkyl group, such as **41**, **42**, and **46**.

Figure 5 depicts the binding model for pyrrolidinyldiamine derivative **31**, in which a ring flip similar to that in **13** (**Fig. 4**) is proposed, extending the carbamate into

Table 4. SAR of R groups of the enantiopure *cis*-(3*R*,4*S*)-pyrrolidinyldiamine derivatives

Compound	R	FXa K_i (nM)	PT EC _{2x} (μM)	Microsomal rate (nmol/min/mg) ^a
25	H	9.5	nd	0.00
28	Fmoc	4.5	nd	nd
29	COMe	0.58	0.94	0.00
33	COEt	2.0	3.2	nd
34	COCHMe ₂	1.3	2.9	0.00
35	CO- <i>t</i> -Bu	1.7	4.5	nd
36	CO-Cyclopropyl	2.1	4.0	nd
37	CO-Phenyl	2.2	9.2	nd
38	COCH ₂ OMe	0.36	3.6	nd
39	COOMe	0.74	3.0	0.00
31	COOEt	0.50	2.1	0.00
40	COOCH ₂ CH ₂ OMe	0.93	2.8	nd
41	SO ₂ Me	0.44	1.6	0.00
42	SO ₂ Et	0.64	3.1	0.00
43	SO ₂ - <i>i</i> -Pr	1.7	3.1	nd
44	CO-N-Pyrrolidinyl	1.7	6.0	nd
45	CONHMe	1.1	2.4	0.00
46	CONMe ₂	0.56	1.8	0.00

^a Based on % remaining after 10-min incubation in human liver microsomes.

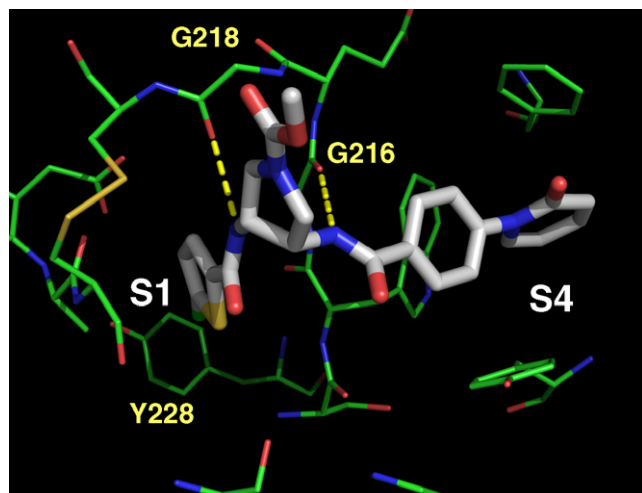


Figure 5. Binding model of the pyrrolidinyldiamide **31** in the active site of FXa showing the carbamate functionality extended into solvent. Created using PyMol.⁸

solvent,¹¹ supporting the similar FXa binding affinity observed in compounds **31** and **1**.

The in vitro liability profile of the pyrrolidinyldiamine compounds (Table 4) was generally good. For instance,

all the compounds tested were very weak against all P450 isozymes (except for the basic pyrrolidinyldiamine **25** showing low μM activity for CYP3A4), non-cytotoxic in the cytotoxicity assay with $\text{IC}_{50} > 100 \mu\text{M}$, and weak against hERG channel (most compounds had hERG flux $\text{IC}_{50} > 80 \mu\text{M}$).¹² Importantly, all the compounds tested in HLM incubation showed improved metabolic stability (100% remaining after 10 min) compared with the cyclopentyl analog **1**.

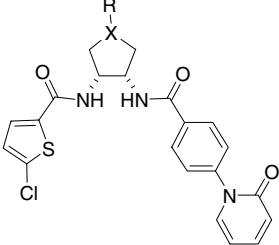
Table 5 illustrates the selectivity profile of example compounds bearing the 4-substituted cyclopentyldiamine, the tetrahydrofuranyldiamine, and the N-substituted pyrrolidinyldiamine cores. In general, these compounds were highly selective against other serine proteases.

Table 6 illustrates the pharmacokinetic properties of selected compounds in dogs. All showed low to moderate V_{dss} . Compared with the corresponding cyclopentyl analog **1**, the tetrahydrofuran **23** and the pyrrolidinyldiamine analogs **29**, **31**, and **42** had increased HLM stability, but higher in vivo clearance. This may be due to a non-metabolic clearance mechanism, such as renal or biliary clearance in vivo, and/or species differences in metabolism. Changing the cyclopentyl core in **1** to the tetrahydrofuran core in **23** improved bioavailability.

Table 5. Selectivity profile of enantiopure 4-substituted cyclopentyldiamine, tetrahydrofuranyldiamine, and 3,4-pyrrolidinyldiamine derivatives

Compound	FXa K_i (nM)	FXIa K_i (nM)	FVIIa K_i (nM)	Chymotrypsin K_i (nM)	Plasma kallikrein K_i (nM)	Trypsin K_i (nM)	Thrombin K_i (nM)	aPC K_i (nM)	Plasmin K_i (nM)	tPA K_i (nM)	Urokinase K_i (nM)
15	0.56	nd	>11,000	>20,000	>10,800	>5000	nd	>21,000	>22,000	>21,000	>14,000
16	1.9	>11,000	>11,000	>20,000	>6000	>5000	>12,000	>21,000	>22,000	>21,000	>14,000
23	2.6	>11,000	>11,000	>20,000	nd	>5000	>12,000	>21,000	>22,000	>21,000	>14,000
29	0.58	10,170	>11,000	>20,000	>6000	>5000	5440	>21,000	>22,000	>21,000	>14,000
31	0.50	7380	>11,000	>20,000	>6000	>5000	4020	>21,000	>22,000	>21,000	>14,000
42	0.64	6680	>11,000	>20,000	>10,800	>5000	3950	>21,000	>22,000	>21,000	>14,000

Table 6. In vitro and dog PK profiles of representative five-membered cyclicdiamines containing phenylpyridone P4 residue

Compound	X	R									
			FXa K_i (nM)	PT EC_{2x} (μM)	Microsomal rate (nmol/min/mg) ^a	Caco-2 P_c (nm/s)	Cl (L/Kg/h) ^b	V_{dss} (L/Kg) ^b	iv $t_{1/2}$ (h)	po $t_{1/2}$ (h) ^c	F% ^c
1	CH_2	—	0.43	1.7	0.063	92	0.7	0.8	0.7	0.7	60
23	O	—	2.6	3.2	0.031	—	1.6	1	1.2	1.2	97
29	N	COMe	0.58	0.90	0.000	<15	1.8	2.4	0.8	0.8	5
31	N	COOEt	0.50	2.1	0.000	25	2.6	2.4	1.4	2.7	25
42	N	SO_2Et	0.64	3.1	0.000	<15	1.5	1.1	0.7	1.3	16

^a Based on % remaining after 10-min incubation in human liver microsomes.

^b iv dose: 0.5 mg/kg.

^c po dose: 0.2 mg/kg.

Table 7. Detailed kinetic parameters for **31**^{a,b}

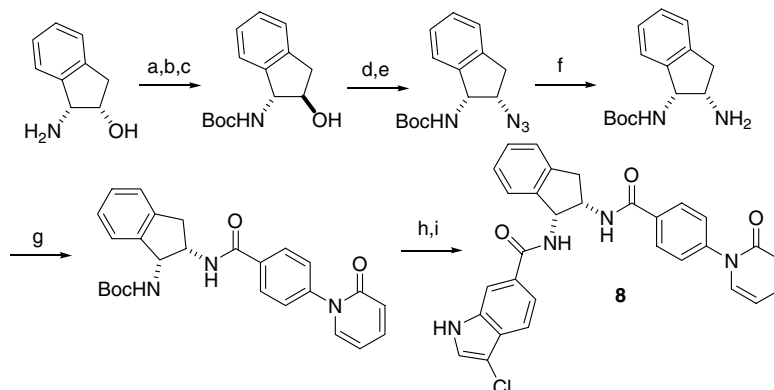
Human Factor Xa parameter	31 Parameter value
25 °C K_i (tripeptide substrate)	0.73 nM
37 °C K_i (tripeptide substrate)	2.6 nM
25 °C K_i (prothrombin)	7.5 nM
37 °C K_i (saturating prothrombin)	30 nM
25 °C Association rate constant	$3.2 \times 10^7 \text{ M}^{-1} \text{ s}^{-1}$
25 °C Dissociation rate constant	$2.3 \times 10^{-2} \text{ s}^{-1}$
37 °C Association rate constant	$2.3 \times 10^7 \text{ M}^{-1} \text{ s}^{-1}$
37 °C Dissociation rate constant	$6.1 \times 10^{-2} \text{ s}^{-1}$

^a K_i 's measured with purified human enzymes and averaged from multiple determinations ($n \geq 2$).

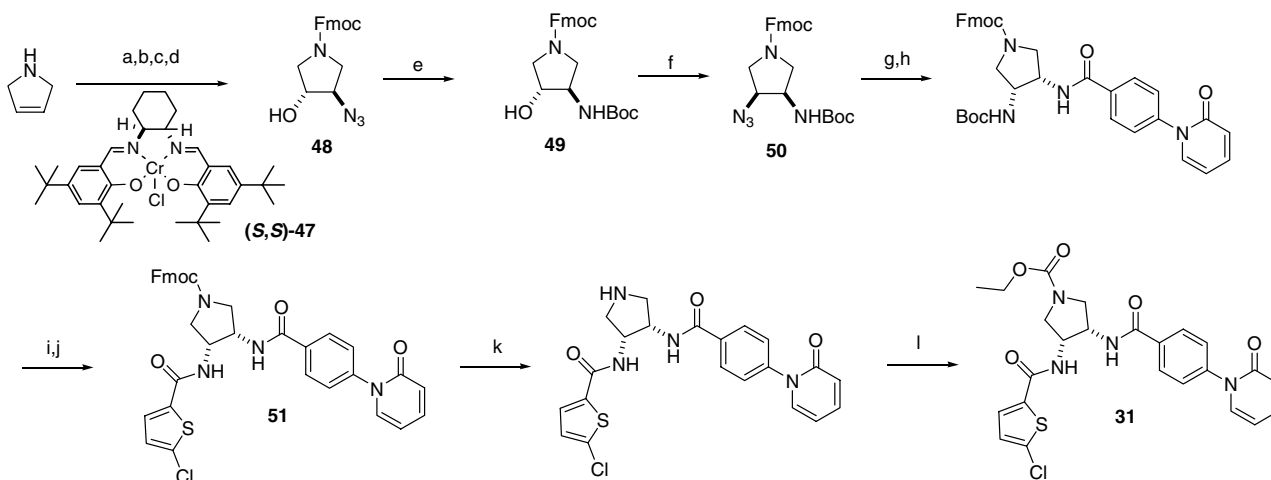
^b Prothrombinase inhibition, association and dissociation rate constants were obtained as described in Ref. 13.

The ethyl carbamate **31** was the only pyrrolidinyldiamine analog having detectable cell permeability (Caco-2 Pc 25 nm/s). As anticipated based on permeability, **31** showed the best oral bioavailability of the pyrrolidinyldiamine compounds ($F\% = 25\%$) and a slightly prolonged $t_{1/2}$ of 1.4 h (iv) and 2.7 h (po) in dogs.

Compound **31** was selected for detailed mechanistic studies and the key kinetic parameters are summarized in Table 7. As predicted for a reversible inhibitor binding in the active site, **31** exhibits competitive inhibition versus a tripeptide chromogenic substrate, but exhibits mixed-type inhibition (with ca. fourfold lower affinity for the ES complex) versus prothrombin, the physiological substrate, which interacts with FXa primarily at exosites.^{13,14} An advantageous consequence of this inhibition mechanism is that **31** is a potent inhibitor at both sub-saturating and saturating levels of prothrombin. Substrate-dependent inhibition mechanisms have also been reported for other FXa inhibitors.^{13,15} At both 25 °C and 37 °C the second-order rate constant for association of **31** with FXa, determined by stopped-flow spectrofluorimetry, is rapid and approaches the diffusion controlled limit. Rapid onset of inhibition of blood coagulation is preferable and has been observed for optimized thrombin¹⁶ and FXa inhibitors.^{13,15b,c,17} Binding of **31** to FXa proceeds by a simple one-step mechanism or by a two-step mechanism with a very weak initial complex (i.e., initial $K_i \gg 5000 \text{ nM}$), since



Scheme 1. Reagents and conditions: (a) $(\text{Boc})_2\text{O}$, Et_3N , THF, 99%; (b) $p\text{-NO}_2\text{C}_6\text{H}_4\text{COOH}$, DEAD, PPh_3 , 57%; (c) NaOMe , CH_3OH , 59%; (d) MsCl , Et_3N , CH_2Cl_2 , 0 °C, 95%; (e) NaN_3 , DMSO, 100 °C, overnight, 47%; (f) H_2 , Pd-C (5%), EtOH, 94%; (g) 4-(2-oxopyridin-1(2H)-yl)benzoic acid, BOP, NMM, DMF, 1 h, 96%; (h) TFA, CH_2Cl_2 , rt, 1 h, 61%; (i) 3-Chloro-L-proline, BOP, NMM, DMF, 37%.



Scheme 2. Reagents and conditions: (a) Fmoc-Cl, DIEA, CH_2Cl_2 , 95%; (b) $m\text{-CPBA}$, NaHCO_3 , CH_2Cl_2 , 60%; (c) TMSN_3 , (*S,S*)-**47** (5 mol%), Et_2O , 89%; (d) 10-CSA (cat.), MeOH, 85%; (e) H_2 , 10% Pd-C, $(\text{Boc})_2\text{O}$, EtOAc, 91%; (f) NaN_3 , H_2SO_4 , H_2O /toluene, 0 °C, then PPh_3 , DEAD, HN_3 , THF, -78 °C to rt; (g) H_2 , 10% Pd-C, EtOH; (h) 4-(2-oxopyridin-1(2H)-yl)benzoic acid, BOP, NMM, THF, 44% for three steps.; (i) 30% TFA, CH_2Cl_2 ; (j) 5-chloro-L-proline, BOP, NMM, THF, 93% for two steps; (k) 10% piperidine, THF, 90%; (l) ClCOOEt , Et_3N , THF, 80%.

plots of the observed rate constants versus inhibitor were linear up to 5000 nM. Dissociation rate constants could thus be calculated from the relationship, $K_i = k_{\text{dissoc}}/k_{\text{assoc}}$, and account for the higher K_i 's at 37 °C. These results are similar to those obtained with both razaxaban and apixaban.¹³

Scheme 1 illustrates the synthesis of enantiopure diaminopyrrolidine derivatives using **8** as an example following the similar sequence as that for compounds **1**.⁶

The synthetic route for enantiopure *cis*-3,4-diaminopyrrolidine core is outlined in **Scheme 2** using the preparation of compound **31** as an example. The 12-step synthesis involved two key reactions. One is the synthesis of the Fmoc protected hydroxylazide pyrrolidine **48** via stereospecific ring opening of the *meso* epoxide with TMS azide catalyzed by Jacobsen's chiral (salen)chromium(III) catalyst **47**.¹⁸ The Fmoc group was chosen as the amino protecting group because it allows high ee and easy monitoring of the reaction progress. The other key transformation is from the *trans* Boc-protected amino alcohol **49** to the *cis* Boc-protected azide **50**. Normal azide formation via sodium azide displacement of the corresponding mesylate in either DMF or DMSO at either room temperature or elevated temperature to 80 °C generated undesirable products, presumably due to the initial Fmoc decomposition followed by other reactions. However, treatment of alcohol **49** with a freshly prepared HN₃ toluene solution under Mitsunobu condition led to the desired *cis* Boc-protected amino azide **50**. Reduction of the crude azide **50**, and then coupling the resulting amine with 4-(2-oxopyridin-1(2*H*)-yl)benzoic acid, followed by deprotection and a subsequent amide formation with 3-chloro-1*H*-indole-6-carboxylic acid afforded the Fmoc protected diaminopyrrolidine **51**. Deprotection of Fmoc group followed by carbamate formation provided compound **31**. Using similar strategies, the tetrahydrofuranyldiamides **23** and **24** were also prepared with an ee >97% measured by chiral analytical HPLC.

In summary, to improve the metabolic stability of the cyclopentylamine derivative **1** while maintaining the sub-nanomolar FXa potency, we synthesized several enantiopure five-membered cyclicdiamine series: the 4-substituted cyclopentylamine, the tetrahydrofuranyldiamine, and the pyrrolidinyldiamine derivatives. Compared with **1**, those compounds having a similarly high FXa potency had an improved metabolic stability in HLM (90–100% remaining after 10 min). The tetrahydrofuranyldiamide **23** had an improved bioavailability in dogs. The ethyl carbamate **31** in the (3*R*,4*S*)-pyrrolidinyldiamine series, having excellent potency and selectivity, and an HLM stability better than **1**, was the best overall compound with a bioavailability of 25% and a $t_{1/2}$ of 2.7 h in dogs.

Acknowledgments

The authors thank Mary F. Grubb for metabolic ID study of compound **1**, and Jeffrey M. Bozarth, Frank

A. Barbera, Tracy A. Bozarth, and Karen S. Hartl for in vitro assays.

References and notes

- Presented in part at the 232nd ACS National Meeting San Francisco, CA, September 10–14, 2006, MEDI-393.
- For review papers of FXa inhibitors, see: (a) Quan, M.; Smallheer, J. *Curr. Opin. Drug Disc. Dev.* **2004**, *7*, 460; (b) Walenga, J. M.; Jeske, W. P.; Hoppensteadt, D.; Fareed, J. *Curr. Opin. Invest. Drugs* **2003**, *4*, 272; (c) Gould, W. R.; Leadley, R. J. *Curr. Pharm. Design* **2003**, *9*, 2337; (d) Quan, M. L.; Wexler, R. R. *Curr. Top. Med. Chem. (Hilversum, Netherlands)* **2001**, *1*, 137.
- (a) Lassen, M. R.; Davidson, B. L.; Gallus, A.; Pineo, G.; Ansell, J.; Deitchman, D. *Blood* **2003**, *102*, 11; (b) Straub, A.; Pohlmann, J.; Lampe, T.; Pernerstorfer, J.; Schlemmer, K.-H.; Reinemer, P.; Perzborn, E.; Roehrig, S. *J. Med. Chem.* **2005**, *48*, 5900; (c) Eriksson, B. L.; Borris, L.; Dahl, O. E.; Haas, S.; Huisman, M. V.; Kakkar, A. K. *J. Thromb. Haemost.* **2006**, *4*, 121; (d) Hampton, T. *JAMA* **2006**, *295*, 743; (e) Wong, P. C.; Crain, E. J.; Watson, C. A.; Zaspel, A. M.; Wright, M. R.; Lam, P. Y. S.; Pinto, D. J.; Wexler, R. R.; Knabb, R. M. *J. Pharmacol. Exp. Ther.* **2002**, *303*, 993.
- Quan, M. L.; Lam, P. Y. S.; Han, Q.; Pinto, D. J.; He, M.; Li, R.; Ellis, C. D.; Clark, C. G.; Teleha, C. A.; Sun, J. H.; Alexander, R. S.; Bai, S. A.; Luetngen, J. M.; Knabb, R. M.; Wong, P. C.; Wexler, R. R. *J. Med. Chem.* **2005**, *48*, 1729.
- Pinto, D. J. P.; Orwat, M. J.; Koch, S.; Rossi, K. A.; Alexander, R. S.; Smallwood, A.; Wong, P. C.; Rendina, R. A.; Luetngen, J. M.; Knabb, R. M.; He, K.; Xin, B.; Wexler, R. R.; Lam, P. Y. S. *J. Med. Chem.* in press.
- Qiao, J. X.; Chang, C.-H.; Cheney, D. L.; Morin, P. E.; King, S. R.; Wang, G. Z.; Wang, T. C.; Rendina, A. R.; Luetngen, J. M.; Knabb, R. M.; Wexler, R. R.; Lam, P. Y. S. *Bioorg. Med. Chem. Lett.* **2007**. doi:10.1016/j.bmcl.2007.06.029.
- Pinto, D.; Quan, M.; Orwat, M.; Li, Y.; Han, W.; Qiao, J.; Lam, P.; Koch, S. PCT Int. Appl. WO 03026652 A1, 2003.
- PyMol. DeLano, W. L. The PyMOL Molecular Graphics System (2002) on World Wide Web <http://www.pymol.org>.
- (a) Knabb, R. M.; Kettner, C. A.; Timmermans, P. B. M. W. M.; Reilly, T. M. *Thromb. Haemost.* **1992**, *67*, 56; (b) Kettner, C. A.; Mersinger, L. J.; Knabb, R. M. *J. Biol. Chem.* **1990**, *265*, 18289.
- Structures **6** and **8** were docked into a representative, in-house crystal structure of FXa using GLIDE XP with refinement using the OPLS-AA force-field and SGB continuum model in the IMPACT module in Maestro. Maestro, version 6.0, Schrödinger, LLC, New York, NY, 2005.
- Structures of compounds **11**, **13**, and **31** were docked with GLIDE XP version 4.0 into a conformationally representative ensemble of crystal structures of the FXa binding site. Top-scoring poses were further refined using the MM-GBSA routine in Maestro in combination with manual modeling. Maestro, version 7.5, Schrödinger, LLC, New York, NY, 2005. For protein ensemble docking see: Cheney, D. L.; Mueller, L. Abstracts of Papers, 229th ACS National Meeting, San Diego, CA, United States, March 13–17, 2005, COMP-307.
- For general descriptions regarding assays for Cyp P450, cytotoxicity, and hERG, please see: (a) Crespi, C. L.; Miller, V. P.; Penman, B. W. *Anal. Biochem.* **1997**, *248*, 188; (b) Graham, F. L.; Smiley, J.; Russell, W. C.; Nairn,

- R., *J. Gen. Virol.* **1977**, 36, 59; (c) Sanguinetti, M. C.; Jurkiewicz, N. K. *J. Gen. Physiol.* **1990**, 96, 195; (d) Sanguinetti, M. C.; Curran, M. E.; Spector, P. S.; Keating, M. T. *Proc. Natl. Acad. Sci.* **1996**, 93, 2208; (e) Trudeau, M. C.; Warmke, J. W.; Ganetzky, B.; Robertson, G. A. *Science* **1995**, 269, 92; (f) Warmke, J. W.; Ganetzky, B. *Proc. Natl. Acad. Sci.* **1994**, 91, 3438.
13. Experimental details for the mechanism studies will be described in a manuscript in preparation on razaxaban and apixaban.
14. Krishnaswamy, S. *J. Thromb. Haemost.* **2005**, 3, 54.
15. (a) Rezaie, A. R. *Thromb. Haemost.* **2003**, 89, 112; (b) Pinto, D. J. P.; Galemme, R. A.; Quan, M. L.; Orwat, M. J.; Clark, C.; Li, R.; Wells, B.; Woerner, F.; Alexander, R. S.; Rossi, K. A.; Smallwood, A.; Wong, P. C.; Luettgen, J. M.; Rendina, A. R.; Knabb, R. M.; He, K.; Wexler, R. R.; Lam, P. Y. S. *Bioorg. Med. Chem. Lett.* **2006**, 16, 5584; (c) Pinto, D. J. P.; Orwat, M. J.; Quan, M. L.; Han, Q.; Galemme, R. A.; Amparo, E.; Wells, B.; Ellis, C.; He, M. Y.; Alexander, R. S.; Rossi, K. A.; Smallwood, A.; Wong, P. C.; Luettgen, J. M.; Rendina, A. R.; Knabb, R. M.; Mersinger, L.; Kettner, C.; Bai, S.; He, K.; Wexler, R. R.; Lam, P. Y. S. *Bioorg. Med. Chem. Lett.* **2006**, 16, 4141.
16. Elg, M.; Gustafsson, D.; Deinum, J. *Thromb. Haemost.* **1997**, 78, 1286.
17. Gould, W. R.; Cladera, E.; Harris, M. S.; Zhang, E.; Narasimhan, L.; Thorn, J. M.; Leadley, R. J., Jr. *Biochemistry* **2005**, 44, 9280.
18. Schaus, S. E.; Larrow, J. F.; Jacobsen, E. N. *J. Org. Chem.* **1997**, 62, 4197.